FEBS Letters 588 (2014) 3751–3760

journal homepage: www.FEBSLetters.org

Removal of both Ycf48 and Psb27 in *Synechocystis* sp. PCC 6803 disrupts Photosystem II assembly and alters Q_A^- oxidation in the mature complex

Simon A. Jackson, John R.D. Hervey, Asher J. Dale, Julian J. Eaton-Rye *

Department of Biochemistry, University of Otago, Dunedin 9016, New Zealand

ARTICLE INFO

Article history:
Received 16 May 2014
Revised 7 July 2014
Accepted 9 August 2014
Available online 27 August 2014

Edited by Richard Cogdell

Keywords:
Assembly
Biogenesis
Photosystem II
Psb27
Synechocystis sp. PCC 6803
Ycf48

ABSTRACT

The Photosystem II (PS II) assembly factors Psb27 and Ycf48 are transiently associated with PS II during its biogenesis and repair pathways. We investigated the function of these proteins by constructing knockout mutants in *Synechocystis* sp. PCC 6803. In ΔYcf48 cells, PS II electron transfer and stable oxygen evolution were perturbed. Additionally, Psb27 was required for photoautotrophic growth of cells lacking Ycf48 and assembly beyond the RC47 assembly complex in ΔYcf48:ΔPsb27 cells was impeded. Our results suggest the RC47 complex formed in ΔYcf48 cells is defective and that this deficiency is exacerbated if CP43 binds in the absence of Psb27.

1. Introduction

Photosystem II (PS II) is a large multi-subunit pigment-protein complex which catalyzes the light-driven oxidation of water and reduction of plastoquinone to plastoquinol [1]. The PS II holoenzyme, located in the thylakoid membrane of oxygenic photoautotrophs, consists of at least 20 polypeptides incorporating a core complex containing the reaction center (RC) D1 and D2 proteins and the chlorophyll *a*-binding proximal antenna proteins CP43 and CP47 [2]. The heterodimeric RC formed by the D1 and D2 proteins binds the majority of the redox active co-factors including the catalytic Mn_4CaO_5 cluster of the oxygen-evolving complex. As a consequence of PS II activity the RC complex is subject to light-induced photodamage resulting in PS II undergoing a constant repair cycle to achieve sustained photosynthetic water splitting [3,4]. Both biogenesis and repair processes of PS II involve the coordinated assembly of many components and pre-assembly complexes [5]. Assembly is assisted by a complement of transiently-associated protein factors that are not found in the mature photosystem [6]. These additional proteins participate in stabilization of pre-assembly complexes and processing of precursor and intermediate forms of the D1 protein (pD1 and iD1, respectively). Two assembly proteins whose functions are not yet understood are Ycf48 and Psb27 [7].

The *Arabidopsis thaliana* homologue of Ycf48, HCF136, is indispensable for PS II assembly [8]. By comparison, a *Synechocystis* sp. PCC 6803 (hereafter *Synechocystis* 6803) Ycf48 knockout mutant displayed reduced PS II assembly and increased sensitivity to photoinhibition because the turnover and replacement of damaged D1 was impaired, suggesting a role for Ycf48 in repair processes [9]. The Ycf48 protein has been identified in isolated preparations of precursor PS II assembly complexes containing pD1 and iD1 up to the CP43-less assembly pre-complex (RC47) in both the so-called PratA-defined membrane (PDM) and thylakoid membrane systems [9,10]. Ycf48 is thought to interact directly with the C-terminal extension of D1 but can still bind in

Abbreviations: Bis–Tris, 2-[bis(2-hydroxyethyl)amino]-2-(hydroxymethyl)-propane-1,3-diol; BSA, bovine serum albumin; BMF, blue measuring flashes; BN-PAGE, blue-native polyacrylamide gel electrophoresis; CP43, 43-kDa chlorophyll *a*-binding protein of the core antenna; CP47, 47-kDa chlorophyll *a*-binding protein of the core antenna; D1, Photosystem II reaction center protein subunit; D2, Photosystem II reaction center protein subunit; DCBQ, 2,6-dichloro-1,4-benzoquinone; DCMU, 3-(3,4-dichlorophenyl)-1,1-dimethylurea; ECL, enhanced chemiluminescence; HEPES, 4-(2-hydroxyethyl)-1-piperazineethanesulfonic acid; iD1, intermediate form of the D1 protein; OCP, orange carotenoid protein; OD, optical density; pD1, precursor form of the D1 protein; PDM, PratA-defined membrane; PS II, Photosystem II; Q_A, primary plastoquinone electron acceptor of PS II; Q_B, secondary plastoquinone electron acceptor of PS II; RC, reaction center; RCII, reaction center pre-complex containing D1, D2, cytochrome b_{559} and Ycf48; RC47, reaction center complex lacking the CP43 protein; RMF, red measuring flashes; SLIC, sequence and ligation independent cloning; TES, N-[tris(hydroxymethyl)methyl]-2-aminoethanesulfonic acid; Tris, 2-amino-2-hydroxymethyl-propane-1,3-diol

* Corresponding author. Fax: +64 3 479 7866.
E-mail address: julian.eaton-rye@otago.ac.nz (J.J. Eaton-Rye).

http://dx.doi.org/10.1016/j.febslet.2014.08.024

the absence of the extension, albeit at reduced levels, suggesting this is not the only factor determining Ycf48 binding [9].

In contrast to Ycf48, there is no evidence for association of Psb27 with the PDM, instead it appears predominantly localized to the thylakoid lumen [10]. Removal of Psb27 from two cyanobacteria, *Thermosynechococcus elongatus* and *Synechocystis* 6803, resulted in mutants that exhibited reduced recovery from high-light-induced photodamage, a consequence of impairment of their PS II repair cycle [11–13]. The role of Psb27 in repair is supported by observations in an *A. thaliana* mutant [14].

Current evidence suggests that Psb27 interacts directly with the CP43 protein and may have a role in stabilizing this subunit as part of a CP43-containing pre-assembly complex prior to its amalgamation with the RC47 complex [13,15–18]. After binding of CP43 to the RC47 complex, but before formation of active PS II monomers or dimers, Psb27 is released allowing subsequent assembly of the Mn_4CaO_5 cluster and binding of the extrinsic subunits [19–21]. In addition, the Psb27 protein is found associated with dimeric CP43-containing complexes specific to the PS II repair cycle that also lack the extrinsic subunits [12].

Given that both Ycf48 and Psb27 proteins bind pre-assembly or repair intermediates of PS II we hypothesized there might be a coordinated role for these subunits; particularly at the point of CP43 integration with RC47. To investigate this possibility we have studied the additive effect of removal of both Ycf48 and Psb27 in *Synechocystis* 6803, allowing us to evaluate their roles in formation and stabilization of PS II.

2. Materials and methods

2.1. Plasmid construction

To generate a construct for inactivation of the *ycf48* ORF (slr2034) sequence and ligation independent cloning (SLIC) was used [22,23]. Overlapping PCR products corresponding to the upstream genomic region, a spectinomycin-resistance cassette (SpecR) [24], downstream genomic region and the pUC19 vector backbone were obtained. The primer pairs: (i) Ycf48_US_fwd and Ycf48_US_rev; (ii) Ycf48_SpecR_fwd and Ycf48_SpecR_rev; (iii) Ycf48_DS_fwd and Ycf48_DS_rev, and (iv) Ycf48_pUC_fwd and Ycf48_pUC_rev, were used to generate these fragments, respectively (Supplementary Table 1). The fragments were subsequently combined in a single SLIC reaction to produce the plasmid pΔYcf48::SpecR.

2.2. Growth of cyanobacterial strains

A sub-cultured derivative of the Williams glucose-tolerant strain of *Synechocystis* 6803, designated GT-01, is referred to throughout as wild type [25,26]. All strains were maintained on solid BG-11 plates (1.5% agar) supplemented with 5 mM glucose, 20 μM atrazine, 10 mM TES-NaOH (pH 8.2), 0.3% sodium thiosulfate and antibiotics (as below). Plates were stored at 30 °C under metal halide lamps at a light intensity of 10 $\mu E\ m^{-2}\ s^{-1}$. Liquid cell cultures were grown mixotrophically in BG-11 containing 5 mM glucose at an illumination level of 50 $\mu E\ m^{-2}\ s^{-1}$ with constant aeration in modified Erlenmeyer flasks according to Eaton-Rye [27]. Where appropriate, growth media contained spectinomycin at 25 $\mu g\ mL^{-1}$ and chloramphenicol at 15 $\mu g\ mL^{-1}$.

2.3. General pre-treatment of cells for physiological measurements

For all physiological characterizations the cells were grown mixotrophically in 300 mL of BG-11 in 500 mL flasks. For each given experiment, 50–100 mL of cells grown to an optical density at 730 nm (OD_{730}) of between 0.8 and 1.2 (measured with a Jasco V-550 UV/Vis spectrophotometer; Jasco, International) were harvested by centrifugation at 2760×*g* for 8 min. Cells were re-suspended in BG-11 with 25 mM HEPES–NaOH (pH 7.5) to a chlorophyll *a* concentration of 5 $\mu g\ mL^{-1}$ (determined as in MacKinney [28]). Twenty milliliters of cell suspension was incubated in a 50 mL conical flask on an orbital shaker at 30 °C at a light intensity of 30 $\mu E\ m^{-2}\ s^{-1}$. After a period of 30 min aliquots of cells were removed and used for the various physiological assays described. Where concentrations of chlorophyll *a* of less than 5 $\mu g\ mL^{-1}$ are specified the cells were diluted immediately prior to the measurements using additional BG-11 HEPES–NaOH (pH 7.5).

2.4. Whole cell absorption spectra

Whole cell absorption spectra were collected using a Jasco V-550 spectrophotometer at a cell density corresponding to an apparent OD at 800 nm of 0.3 with Scotch tape affixed in both the sample and reference optical paths. An absorption scan, against a reference sample of BG-11, was performed using a slit width of 1 nm.

2.5. Oxygen evolution assays

Oxygen evolution measurements were performed in 1 mL volumes using a Clarke-type electrode (Hansatech, UK) maintained at 30 °C by a recirculating water bath. Samples were measured at a chlorophyll *a* concentration of 5 $\mu g\ mL^{-1}$ in the presence of 0.2 mM 2,6-dichloro-1,4-benzoquinone (DCBQ) and 1 mM potassium ferricyanide ($K_3[Fe(CN)_6]$). Illumination of the samples was provided by an FLS1 light source (Hansatech, UK) equipped with a 580 nm long-pass filter (Melles Griot, USA) and fiber optic cable assembly. The photon flux output at the chamber end of the cable was 8000 $\mu E\ m^{-2}\ s^{-1}$. Data presented are for a minimum of five total replicates, gathered from at least three independent experiments. Rates were determined on the basis of the initial slope up to 30 s after the illumination began.

2.6. Low temperature (77 K) fluorescence emission spectra

For measurement of fluorescence emission at 77 K a modified MPF-3L fluorescence spectrometer (Perkin Elmer, USA.) equipped with a custom made liquid nitrogen Dewar was used. Five hundred microliter samples of light-adapted cells at a chlorophyll *a* concentration of 2.5 $\mu g\ mL^{-1}$ were snap frozen, using liquid nitrogen, in glass tubes (6 mm outer diameter, 4 mm inner diameter). For data collected at an excitation peak of 440 nm the excitation and emission slit widths were set at 12 and 2 nm, respectively. At an excitation peak of 580 nm, slit widths of 8 and 2 nm were used. Emission spectra were collected at a scan rate of approximately 100 $nm\ min^{-1}$. For each strain 3–4 independent experiments, each consisting of two technical replicates were performed and data averaged. Normalization of the spectra were performed on the basis of baseline subtraction and normalization to the maxima of PS I emission at 725 nm.

2.7. Room temperature variable chlorophyll a fluorescence measurements

All room temperature variable chlorophyll *a* fluorescence measurements were made using a FL-3300 fluorometer (PSI instruments, Czech Republic) equipped with blue light emitting diodes (455 nm peak wavelength) for actinic illumination. Probe flashes employed either a blue measuring flash (BMF, 455 nm) or red measuring flash (RMF, 625 nm), each with a 3 μs duration. Samples consisted of 2 mL of cells at a chlorophyll *a* concentration of 2 $\mu g\ mL^{-1}$

and were dark adapted for 5 min prior to measurement. Where indicated, 3-(3,4-dichlorophenyl)-1,1-dimethylurea (DCMU) was added 2 min after commencement of dark adaptation at a final concentration of 50 μM. For the fluorescence induction protocol four BMF or RMF pulses spaced at 200 ms intervals were used to determine the F_o level before the blue actinic light (set at 50% intensity) was commenced. A logarithmic series of BMF or RMF was used to probe fluorescence induction in the 68 μs to 10 s timescale. For the fluorescence relaxation experiments a series of four BMF spaced at 200 ms intervals were used to determine the F_o level. This was followed 200 ms later by a 30 μs saturating actinic flash, and then a logarithmic series of BMF. The first data point used for analysis was 100 μs after the end of the actinic flash. For kinetic analyses of fluorescence relaxation in the absence of DCMU data up to 50 s were used, while in its presence the data sets were truncated to 10 s. Kinetic analyses were performed according to models previously described [29]. A correction was applied to account for the non-linear relationship between fluorescence and the Q_A oxidation state [30]. In the absence of DCMU, a correction was also applied for the oxidation of Q_A prior to the first data point measured.

2.8. Preparation of thylakoid membranes

Cells were grown as described for physiological experiments, harvested and re-suspended in isolation buffer (50 mM HEPES–NaOH (pH 7.2), 10 mM $MgCl_2$, 5 mM $CaCl_2$ and 1 M sucrose, 1 mM ε-caproic acid, 1 mM phenylmethylsulfonyl fluoride, and 2 mM benzamidine). Cells were incubated on ice for 30 min in the dark before disruption using a Mini-Beadbeater (BioSpec Products, Inc., USA). Five cycles of bead beating (20 s each with 5 min rests on ice) were applied using a half volume of 0.1 mm diameter zirconia beads. Beads and unbroken cells were removed by centrifugation twice at 7500×*g* for 5 min. Thylakoids were then pelleted by centrifugation at 60 000×*g* for 30 min at 4 °C, and re-suspended in isolation buffer, pelleted again and finally re-suspended in solubilization buffer (25 mM Bis–Tris–HCl (pH 7.0), 20% w/v glycerol and 0.25 mg L^{-1} Pefabloc SC). Isolated thylakoids were frozen in liquid nitrogen and stored at −80 °C.

2.9. Blue-native polyacrylamide gel electrophoresis and Western blotting

Thylakoid membranes at a concentration of 0.5 mg chlorophyll *a* per mL were solubilized by incremental addition of 0.5 volumes of solubilization buffer containing 3% β-dodecyl maltoside (Anatrace, USA) (1/5 volume every 2 min) and incubated on ice for a further 10 min. Insoluble material was removed by centrifugation at 15 000×*g* for 15 min. Samples containing 2 μg chlorophyll *a* equivalent of solubilized material were loaded on to precast 3–12% Bis–Tris gradient gels (Life Technologies, USA) and run at 4 °C. For western blotting and immunodetection the proteins were transferred to polyvinylidene difluoride membrane via electroblotting at 15 V for 3 h at 4 °C in buffer containing 25 mM Tris, 192 mM glycine, 10% v/v methanol and 0.05% w/v sodium dodecyl sulfate. Membranes were destained in methanol then blocked using 4% BSA. The primary antibodies for the PsbA (D1), PsbB (CP47) and PsbC (CP43) subunits were obtained from Agrisera, Sweden. The secondary antibody (Sigma, USA) was conjugated to peroxidase for detection using enhanced chemiluminescence (ECL). Detection was performed using a CCD detector system (Fuji imager PS3000) by incubating the membrane in freshly prepared ECL reagent (Abcam, UK).

3. Results

3.1. Construction and verification of mutants

The *Synechocystis* 6803 genome encodes one copy of a *ycf48* homologue (slr2034). Transcript analysis suggests the slr2034 ORF is part of an operon with an upstream ORF encoding for a rubredoxin protein (RubA) (Fig. 1A) [31,32]. In *Synechocystis* 6803 the tandem *rubA-ycf48* genes are located immediately upstream of the *psbEFLJ* operon, a gene arrangement also found in many other cyanobacteria (Supplementary Table 2). To inactivate the *ycf48* ORF a construct was designed to introduce a spectinomycin-resistance cassette 515 bp downstream of the start codon (see Section 2). In addition, the *psb27* ORF (slr1645) was interrupted by the introduction of a chloramphenicol-resistance cassette at

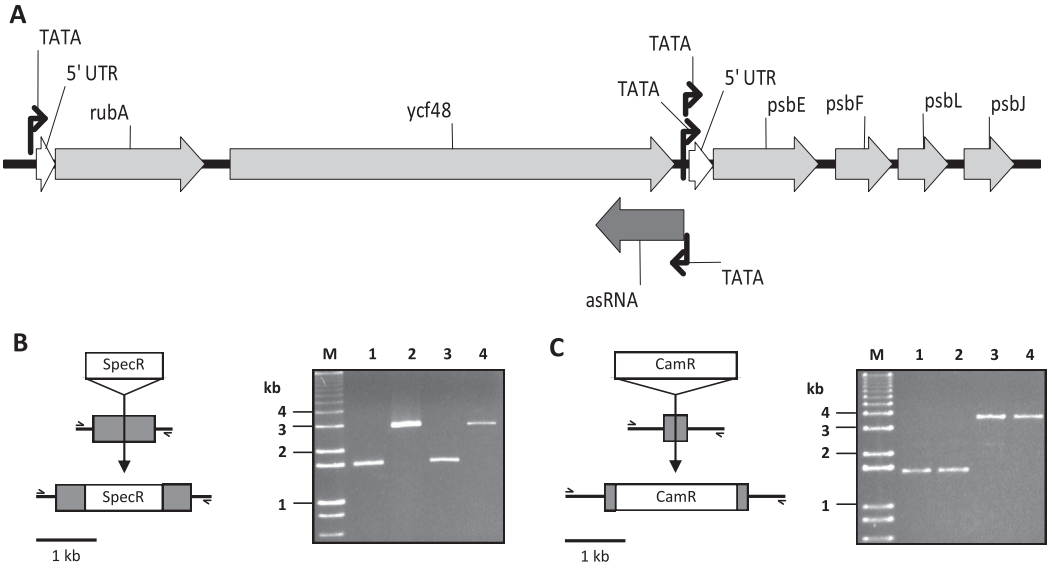

Fig. 1. Operon structure and segregation analysis. (A) Arrangement of the *rubA* and *ycf48* genes and the *psbEFLJ* operon in *Synechocystis* 6803. (B) Confirmation of segregation by PCR for the inactivation of *ycf48* by insertion of a 1.3-kb spectinomycin-resistance cassette (SpecR). (C) Confirmation of segregation by PCR for inactivation of *psb27* by insertion of a 2.1-kb chloramphenicol-resistance cassette (CamR). Lanes in B and C are molecular weight marker (M), wild type (1), ΔYcf48 (2), ΔPsb27 (3) and ΔYcf48:ΔPsb27 (4).

an intragenic ClaI site using a plasmid developed by Bentley et al. [33]. This strategy allowed for the construction of both single ΔYcf48 and ΔPsb27 mutants and a ΔYcf48:ΔPsb27 double mutant. Colony PCR was performed to check integration and segregation of the constructs (Fig. 1B and C).

3.2. Photoautotrophic growth and oxygen evolution are blocked in the ΔYcf48:ΔPsb27 strain

Under the conditions tested, inactivation of the *ycf48* ORF impaired photoautotrophic growth, increasing the doubling time from 11.5 h (wild type) to 21.7 h (ΔYcf48) (Fig. 2A). Removal of Psb27 only slightly reduced the photoautotrophic growth rate (13.8 h) compared to wild type. However, the removal of Psb27 from the ΔYcf48 strain resulted in severe loss of photoautotrophic growth capacity (exhibiting an initial doubling time of 35.5 h).

Removal of Ycf48 in the wild-type background reduced the saturated rate of steady-state oxygen evolution, measured in the presence of DCBQ and $K_3[Fe(CN)_6]$, by approximately 52% (281 versus 592 μmol O_2 per mg chlorophyll *a* per h for wild type) (Table 1).

Table 1
Oxygen evolution rates.[a]

	(μmol O_2 mg Chl a^{-1} h^{-1})
Wild type	592 ± 74
ΔYcf48	281 ± 55
ΔPsb27	585 ± 83
ΔYcf48:ΔPsb27	165 ± 10

[a] Oxygen evolution was measured in the presence of DCBQ and $K_3[Fe(CN)_6]$ as described in Section 2.

The ΔPsb27 strain was able to evolve oxygen at a comparable level to wild type, giving a rate of 585 μmol O_2 per mg chlorophyll *a* per h. The depressed oxygen evolution capacity observed in the ΔYcf48 strain was compounded by removal of Psb27, resulting in a 72% reduction compared to wild type. Additionally, inactivation of *ycf48* resulted in an apparent susceptibility to photoinactivation during the time course of the assay, again exacerbated by removal of the Psb27 subunit but not evident for the wild type or the Psb27 knockout strain (Fig. 2B).

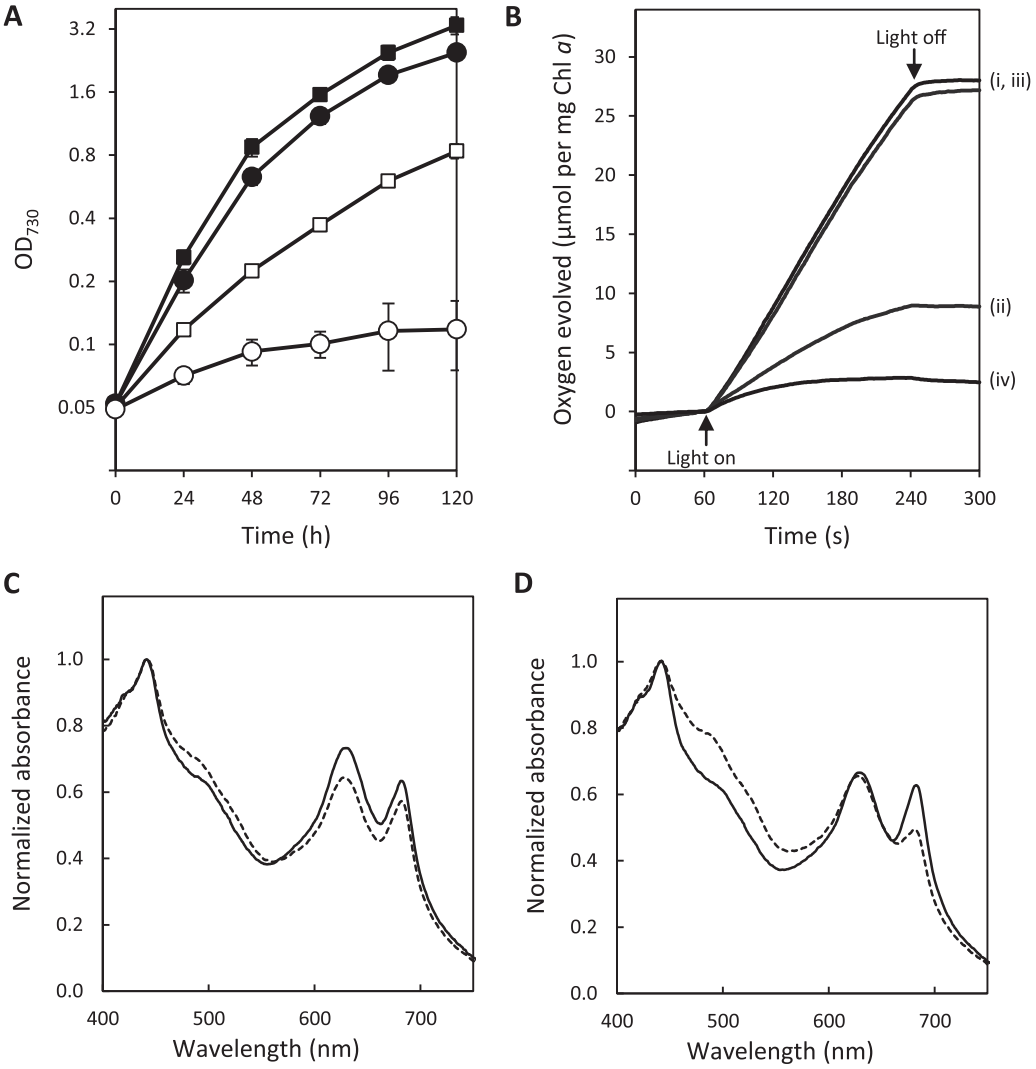

Fig. 2. Removal of Psb27 in a ΔYcf48 strain retards photoautotrophic growth and oxygen evolution and modifies the whole-cell absorption spectrum. (A) Photoautotrophic growth curve determined by light scattering at 730 nm: wild type (solid squares), ΔYcf48 (open squares), ΔPsb27 (solid circles) and ΔYcf48:ΔPsb27 (open circles). Error bars represent the standard error from at least 3 independent experiments. (B) Oxygen evolution traces: wild type (i), ΔYcf48 (ii), ΔPsb27 (iii) and ΔYcf48:ΔPsb27 (iv). (C) Whole cell absorption spectra: wild type (solid line) and ΔYcf48 (dotted line). (D) Whole cell absorption spectra: ΔPsb27 (solid line) and ΔYcf48:ΔPsb27 (dotted line). In C and D, spectra are the average of three independent experiments and are normalized to the maxima at 435 nm.

During the growth curve measurements we noted a difference in the coloration of the strains lacking Ycf48 relative to wild type. To examine this further we analyzed the cellular pigment composition for each of the strains by room temperature absorption measurements. On a whole-cell basis the ΔYcf48 strain exhibited a small increase in the absorption region associated with carotenoids (475–520 nm) and a decrease in the absorption maxima at 625 and 680 nm (Fig. 2C). Aside from a minor decrease in the 625 nm peak there was no notable alteration in pigment content for the ΔPsb27 strain relative to wild type (Fig. 2C and D). However, in the absence of Ycf48 the effect of Psb27 removal resulted in large increases in the carotenoid absorption region and suppression of the 680 nm peak that originates from absorption by chlorophyll *a* (Fig. 2D).

3.3. Low temperature (77 K) fluorescence emission spectra

A reduction in the oxygen evolution capacity, referenced on a chlorophyll *a* basis, might be attributable to a change in the assembly levels of PS II. We therefore evaluated the ratio between PS II and PS I in each of the strains by performing low temperature (77 K) fluorescence emission experiments using an excitation beam with a peak wavelength of 440 nm that specifically targets chlorophyll *a* (Fig. 3A and B). When the spectra are normalized to the PS I maxima at 725 nm, inactivation of the *ycf48* gene in the wild-type background resulted in a reduction of emission at both 685 and 695 nm and a small increase in the amplitude of the 685 nm peak relative to the 695 nm peak (Fig. 3A). These peaks at 685 and 695 nm are typically assigned to the CP43 and CP47 primary antenna subunits of PS II, respectively, but several other complexes might be responsible for the 685 nm emission peak: including, but not limited to, IsiA or unassembled CP43- or CP47-containing complexes [34,35]. For the ΔPsb27 strain the emission spectra showed a reduction in the amplitudes of both the 685 and 695 nm peaks, this time with the 685 nm peak more reduced compared to the 695 maxima (Fig. 3B). Inactivation of the *psb27* gene in the Ycf48 knockout background induced substantial changes to the 77 K fluorescence emission spectra, including a large increase in the 685 nm peak and a concomitant reduction in the 695 nm shoulder (Fig. 3B).

Examination of 77 K fluorescence emission spectra collected at an excitation wavelength targeting phycobillisome pigments (580 nm) revealed differences in phycobillisome-coupled energy distribution for each of the mutant strains (Fig. 3C and D). Removal of Ycf48 in the wild-type background resulted in an increase in the spectral maxima observed at 680 nm, along with small reductions in the 649 and 664 nm peaks (Fig. 3C). For the ΔPsb27 strain the 680 nm peak was distinctly reduced compared to that in wild type, both in respect to its amplitude and relative level compared to the 649 and 664 nm peaks (Fig. 3C and D). For the ΔYcf48:ΔPsb27 strain the opposite effect was observed, whereby the 680 nm peak

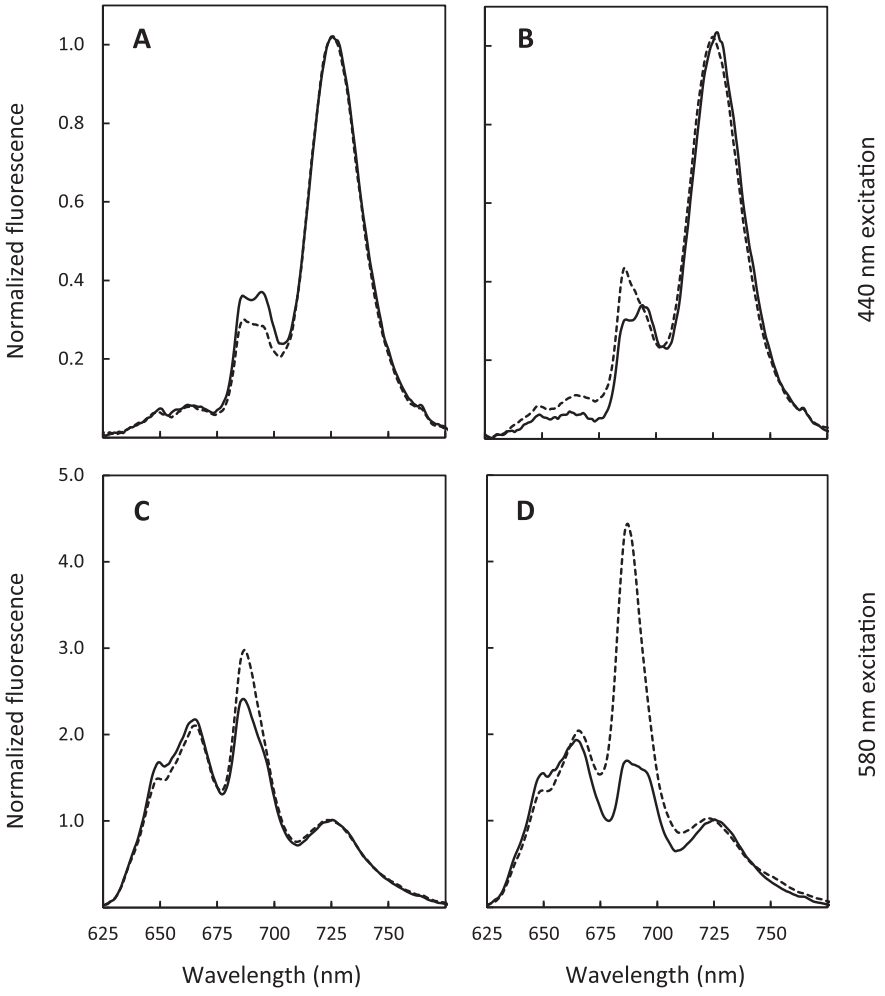

Fig. 3. 77 K fluorescence emission spectra. (A) 440 nm excitation for wild type (solid line) and ΔYcf48 (dotted line). (B) 440 nm excitation for ΔPsb27 (solid line) and ΔYcf48:ΔPsb27 (dotted line). (C) 580 nm excitation for wild type (solid line) and ΔYcf48 (dotted line). (D) 580 nm excitation for ΔPsb27 (solid line) and ΔYcf48:ΔPsb27 (dotted line). Spectra are the average of at least 3 independent experiments and are normalized to the PS I emission maxima.

displayed a much higher emission than wild type or the parent ΔYcf48 strain.

3.4. Variable chlorophyll a fluorescence measurements

The charge separation and recombination characteristics of PS II centers in each strain were investigated with a series of experiments examining fluorescence induction and decay. Inactivation of *ycf48* induced a significant reduction in variable fluorescence relative to wild type when measured in the presence or absence of DCMU with either BMF or RMF (Fig. 4A–D). The BMF examine the Q_A oxidation state by direct probing of chlorophyll fluorescence, while RMF provide phycobillisome-coupled fluorescence emission. Comparison of the two provides information on energy partitioning to complement the low temperature steady-state fluorescence data. It should be noted that the amplitudes of fluorescence presented are arbitrary and specific to the optical configuration of the fluorometer, in addition the relative amplitudes of data obtained with BMF versus RMF are not directly comparable as these are dependent on the flash intensity and gain settings.

For the ΔYcf48 strain the maximum amplitude of variable fluorescence (F_V, defined as $F–F_o$) was reduced to less than 50% of wild

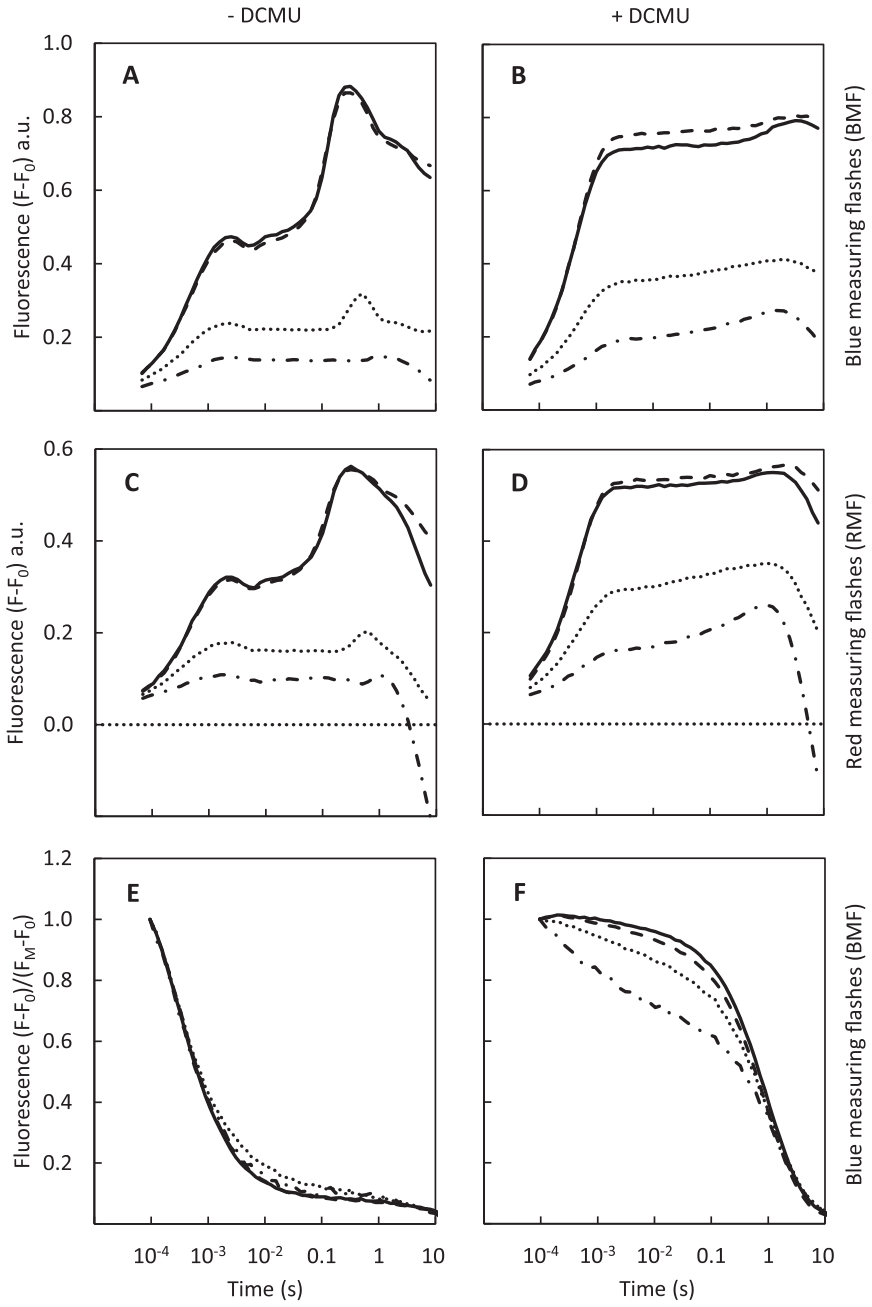

Fig. 4. Room temperature fluorescence induction and relaxation of fluorescence following single-turnover actinic flashes. (A–D) Room temperature fluorescence induction observed upon illumination of dark-adapted cells with a constant actinic light. Strains are: wild type (solid), ΔYcf48 (dots), ΔPsb27 (dashes) and ΔYcf48:ΔPsb27 (dash-dots) in the absence (panels A and C) and presence (panels B and D) of DCMU. In all instances constant blue (455 nm) illumination was used with either blue (panels A and B) or red (625 nm) measuring flashes. The time scale is relative to the commencement of illumination. For clarity the *x*-axis in panels C and D is displayed equivalent to minus 0.2 on the *y*-axis, the actual zero $F–F_o$ level is shown with a dotted horizontal line. (E) Relaxation of fluorescence following single-turnover actinic flashes in the absence of DCMU. (F) Relaxation of fluorescence following single-turnover actinic flashes in the presence of DCMU. In panels E and F the strains are: wild type (solid), ΔYcf48 (dots), ΔPsb27 (dashes) and ΔYcf48:ΔPsb27 (dash-dots). Data displayed are for the average of at least 3 independent experiments.

Table 2
Dark-adapted background (F_o) fluorescence data.[a]

	BMF (a.u.)	RMF (a.u.)
Wild type	0.501 ± 0.027	0.734 ± 0.050
ΔYcf48	0.495 ± 0.017	0.799 ± 0.026
ΔPsb27	0.456 ± 0.020	0.509 ± 0.021
ΔYcf48:ΔPsb27	0.599 ± 0.027	1.404 ± 0.086

[a] The amplitudes between BMF and RMF are not directly comparable. Data shown were collected in the absence of DCMU. No significant difference was observed in its presence.

type when accessed using both BMF and RMF. The ΔPsb27 strain exhibited similar fluorescence induction characteristics to wild type for all conditions examined but inactivation of the *psb27* gene in the absence of Ycf48 exacerbated the depression of variable fluorescence observed for the ΔYcf48 strain. In addition, the characteristic J-P rise [36], observed in the absence of DCMU, was lost in the ΔYcf48:ΔPsb27 strain. The amplitude of the fluorescence in the P region was observed to change with addition of DCMU and interestingly for wild type as well as the ΔPsb27 strain, the fluorescence yield was similar or reduced in the presence of DCMU while in the ΔYcf48 and ΔYcf48:ΔPsb27 strains the yield was increased by addition of DCMU.

In all strains the fluorescence observed using RMF decreased after the *P* peak was reached but for the ΔYcf48:ΔPsb27 strain the reduction was accelerated, with the fluorescence dropping below the initial F_o level; equivalent to zero on the *y*-axis for the F–F_o data displayed. The F_o data cannot be displayed on these figures as they occur prior to the start of the time-scale (x) axis (referenced to the activation of actinic illumination) but are presented in Table 2. No appreciable difference between the F_o for all strains was observed using BMF but when using RMF the F_o level was decreased in ΔPsb27 and considerably elevated in the ΔYcf48:ΔPsb27 strain. An increase in F_o would reduce the F_V/F_M parameter that is classically quoted to illustrate PS II functionality but the underlying cause of the F_o increase in the double mutant might be independent of PS II. Therefore we have presented F–F_o during the time course of the assay as a more accurate representation of PS II activity, particularly given the observation that toward the end of the measurements F drops below the initial F_o in our data. This effect has previously been linked to alterations in PBS coupling during the fluorescence induction assay [37].

The decay of variable fluorescence following a single turnover saturating flash (455 nm) was measured using a BMF in the absence and presence of DCMU (Fig. 4E and F). For each of the strains the decay kinetics corresponding to the reoxidation of Q_A^- were analyzed and these are summarized in Table 3. In the absence of DCMU the ΔYcf48 strain exhibited a similar fast phase to wild type but showed a decreased rate for the middle phase and increased rate and amplitude for the slow phase. For the ΔPsb27 strain the kinetics of Q_A^- oxidation observed were similar to wild type. The ΔYcf48:ΔPsb27 strain showed a large increase in the rate of the fast phase but with slightly reduced amplitude compared to wild type. The decrease in the rate of the middle phase observed in ΔYcf48 was reversed by removal of Psb27, resulting in a faster rate than wild type but the increase in the rate and amplitude of the slow phase was retained.

In the presence of DCMU the oxidation of Q_A^- for wild type was dominated by a slow phase (modeled as a hyperbolic component) with a rate constant of ~1.4 s, with an additional exponential component (fast phase) present at negligible levels (Table 2). For the ΔPsb27 strain the slow component also dominated, with only a minor increase in the fast phase compared to wild type. For the ΔYcf48 strain the amplitude of the fast component increased to 7.4 ± 1.0%, apparent as a small increase in the initial decay of the fluorescence relaxation curve (Fig. 4F). The ΔYcf48:ΔPsb27 strain exhibited a large increase in the initial relaxation of fluorescence, corresponding with an approximately fourfold increase in the rate, and fivefold increase in the amplitude, of the fast kinetic component of Q_A^- oxidation compared to wild type.

3.5. Assembly of PS II complexes

Assembly of PS II complexes was analyzed by blue-native polyacrylamide gel electrophoresis (BN-PAGE) followed by western blotting (Fig. 5). The removal of Ycf48 did not preclude assembly of the three predominant macromolecular PS II complexes found in wild type (dimers, monomers and CP43-less monomers) but the level of assembly, particularly of the dimer complex, was reduced. In contrast, removal of the Psb27 subunit did not appear to impair assembly relative to wild type. However, the double mutant lacking both Ycf48 and Psb27 was largely unable to assemble beyond the RC47 (CP43-less monomer) stage. Furthermore, there was an enhanced accumulation of low-molecular-weight complexes which showed reactivity with the α-CP43 antibody in the ΔYcf48:ΔPsb27 strain.

4. Discussion

4.1. A requirement for Psb27 in the absence of Ycf48

Inactivation of either *ycf48* or *psb27* in *Synechocystis* 6803 does not prevent photoautotrophic growth and for the wild-type and ΔPsb27 strains similar phenotypes are found when physiological measurements are performed on whole cells grown in BG-11 medium [9,13,19,33]. However, the combination of high light and low temperature has been shown to prevent photoautotrophic growth of a *T. elongatus* ΔPsb27 mutant [12].

Bentley et al. [33] reported that a ΔPsbM:ΔPsb27 double mutant was an obligate photoheterotroph; however, we have recently sequenced the entire genome of this strain and identified a spontaneous mutation in the second transmembrane helix of

Table 3
Kinetic analysis of Q_A^- oxidation.[a]

No addition	Fast phase ($t_{1/2}$/amplitude)	Middle phase ($t_{1/2}$/amplitude)	Slow phase ($t_{1/2}$/amplitude)
Wild type	616 μs (±11)/60% (±1.1)	6.7 ms (±0.2)/26% (±1.2)	8.5 s (±1.9)/13% (±0.8)
ΔYcf48	678 μs (±37)/57% (±1.3)	15.0 ms (±3.3)/26% (±2.7)	4.8 s (±1.3)/18% (±1.5)
ΔPsb27	648 μs (±22)/60% (±0.4)	7.7 ms (±0.5)/27% (±0.6)	8.0 s (±1.4)/13% (±0.5)
ΔYcf48:ΔPsb27	487 μs (±65)/54% (±1.1)	5.2 ms (±0.5)/29% (±1.1)	4.7 s (±1.5)/16% (±0.7)
with DCMU	Fast phase ($t_{1/2}$/amplitude)	Slow phase ($t_{1/2}$/amplitude)	
Wild type	7.9 ms (±1.1)/2.6% (±0.2)	1.36 s (±0.11)/97.4% (±0.2)	
ΔYcf48	5.8 ms (±1.5)/7.4% (±1.0)	1.55 s (±0.09)/92.6% (±1.0)	
ΔPsb27	6.7 ms (±0.8)/3.9% (±0.2)	1.27 s (±0.06)/96.1% (±0.2)	
ΔYcf48:ΔPsb27	2.2 ms (±0.2)/14.9% (±1.5)	1.70 s (±0.10)/85.1% (±1.5)	

[a] Kinetic analysis was performed on corrected fluorescence relaxation curves following a saturating single turnover flash in the absence or presence of DCMU as described in Section 2.

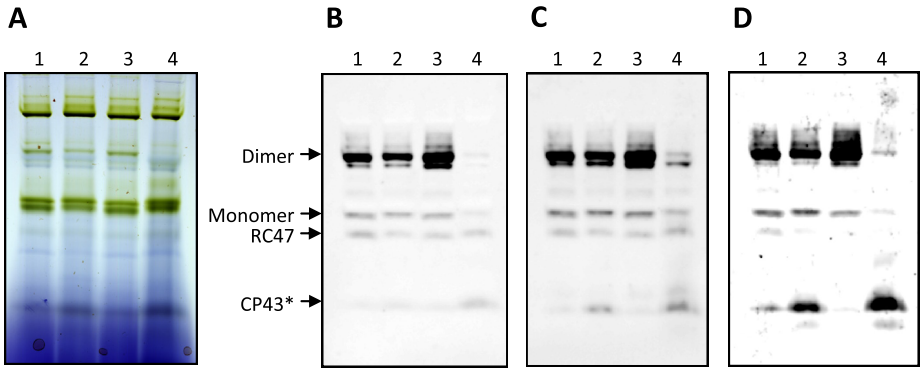

Fig. 5. Analysis of PS II assembly. Solubilized thylakoid membranes run on BN-PAGE (A) followed by western blotting using antibodies for the D1 (B) CP47 (C) and CP43 (D) subunits. Lanes are wild type (1), ΔYcf48 (2), ΔPsb27 (3) and ΔYcf48:ΔPsb27 (4).

CP43 (Gly116 to Asp substitution) in the original ΔPsbM:ΔPsb27 mutant; a new ΔPsbM:ΔPsb27 strain created without this mutation is capable of photoautotrophic growth (data not shown). Hence the requirement of Psb27 in the ΔYcf48 strain in Fig. 2 presents a novel observation where the Psb27 protein is essential to support sustained photoautotrophic growth and oxygen evolution in *Synechocystis* 6803 under standard growth conditions.

4.2. Is there an assembly bottleneck in the ΔYcf48:ΔPsb27 mutant?

The impaired growth of the ΔYcf48 strain correlated with a reduced level of PS II assembly as seen by the increased PS I/PS II ratio in Fig. 3A, a reduced PS II specific variable fluorescence (F–F_o using BMF) in Fig. 4A and B and the diminished levels of PS II monomers and dimers detected in Fig. 5. Likewise PS II assembly is severely restricted in the ΔYcf48:ΔPsb27 double mutant. In addition, the reduced levels of assembled PS II in both strains is accompanied by these mutants accumulating sub-complexes containing CP43 and CP47 (Fig. 5C and D). Isolated early assembly sub-complexes containing CP43 or CP47 have previously been shown to both exhibit 77 K fluorescence emission at a peak of 685 nm which might explain the increase in this peak observed in the ΔYcf48:ΔPsb27 cells [35].

Ycf48 has been shown to be associated with both an early assembly complex containing pD1 and a D1/D2 assembly intermediate (RCII) complex which goes on to form RC47 by combining with the CP47 pre-complex [9,38,39]. At this stage the Ycf48 protein is believed to have dissociated and a CP43 pre-assembly complex containing Psb27 binds to give an inactive monomeric PS II [13,17,38,40]. A previously reported double mutant lacking both the Ycf48 and sll0933 assembly factors displayed phenotypes dominated by the absence of Ycf48 and on the basis of these observations it was deduced that sll0933 functions later in the assembly process [41]. The observation of an additive effect in the ΔYcf48:ΔPsb27 double mutant is thus of particular importance because the association of the Psb27-containing CP43 pre-complex with RC47 is currently thought to be after the action and dissociation of Ycf48; if the impairment of CP43 incorporation into RC47 resulted wholly from the absence of Psb27 then the ΔPsb27 strain would show reduced PS II assembly. As such, our observations imply a direct interaction between complexes containing Ycf48 with those containing Psb27.

In this study cells were grown under a continuous light regime and characterized during the logarithmic phase of growth. Therefore the PS II pool will be a mixed population with a portion representing de novo biogenesis and the remainder in constant flux between mature functioning centers and those undergoing repair following photodamage. In the PS II repair cycle, CP47, along with several other subunits, remains associated with the core D2-cytochrome b_{559} component of RCII while newly synthesized D1 is incorporated (reviewed in Mabbitt et al. [7]). Hence the Psb27-containing CP43 subunit is incorporated directly after D1 addition without the intermediate step of CP47 binding. This process, along with D1 processing, may be partially coordinated by the Ycf48 and Psb27 assembly factors.

4.3. Centers formed in the ΔYcf48 and ΔYcf48:ΔPsb27 mutants are functionally distinct

The ΔYcf48 and ΔYcf48:ΔPsb27 strains remained capable of evolving oxygen, albeit at reduced rates, indicating that assembly can proceed beyond the "bottleneck" in the biogenesis and repair pathways. Even in the double mutant the initial rate of PS II-specific oxygen evolution supported by DCBQ was ~28% of the rates observed in wild type or the ΔPsb27 strain; however, the activity rapidly decreased during the assay suggesting an enhanced sensitivity to photoinactivation. One possible explanation is that the PS II centers are receiving too much light as a result of an increased antenna to PS II center ratio. We explored this possibility by investigating phycobillisome connectivity in the 580 nm fluorescence emission spectra (Fig. 3D). The increased emission from PBS specific fluorophores suggests that many phycobilisomes are not coupled to photosystem centers (PS I or PS II) in the ΔYcf48:ΔPsb27 strain, thereby contradicting this hypothesis.

To investigate if the susceptibility to photoinactivation arose from functional impairment of PS II centers we examined the effect of a single turnover flash on PS II electron transfer. In ΔYcf48 cells there was an increase in the millisecond component suggesting an altered Q_B site [42]. Moreover, in the ΔYcf48:ΔPsb27 strain an enhanced millisecond component associated with Q_A^- oxidation was observed in the presence of DCMU that appeared to "compete" with the slowed millisecond component in the single ΔYcf48 strain detected in the absence of DCMU (Table 3). This may indicate that side-path electron transfer through cytochrome b_{559}, potentially involving β-carotene and chlorophyll Z on D2, is active in assembled PS II centers formed in the absence of Ycf48 and Psb27 [43]. Alternatively, there may be enhanced recombination with $P680^+$. These observations suggest that although PS II assembly can proceed beyond the assembly bottleneck in these mutants the resulting centers are in fact compromised and might possibly be more susceptible to photodamage. This increased light sensitivity has previously been demonstrated for Ycf48 knockout strains and linked to photoinactivation [9,41]. Hence the inability of the double mutant to sustain photoautotrophic growth may arise from both an increased susceptibility to photodamage and a retarded assembly pathway during both biogenesis and repair.

In support of this theory is the accumulation of pigments absorbing in the carotenoid region of the whole cell absorption

spectra (Fig. 2C and D). Carotenoids, which play an important role in photoprotection of PS II, are found not only in mature centers but also in early assembly complexes of CP43 and CP47 [35]. Interestingly the orange carotenoid protein (OCP), a carotenoid-containing protein complex involved in photoprotection, absorbs in the same region with a maximal absorbance peak at 510 nm for the active form [44]. Furthermore, OCP is known to associate with phycobillisomes, pointing to coordination between phycobillisome coupling, regulation of photoprotection and energy distribution during the early stages of PS II biogenesis and repair.

4.4. Concluding remarks

While removal of Psb27 alone does not readily impair PS II performance in *Synechocystis* 6803, a clear role for Psb27 is observed in the absence of Ycf48. This requirement for Psb27 may be heightened in vivo if environmental factors adversely affect the production of D1 during recovery from photodamage. Although Ycf48 is not absolutely required for PS II biogenesis the centers formed in the absence of Ycf48 are compromised and the extent of this disruption appears to be partly compensated for by the presence of Psb27.

Acknowledgements

S.A.J. was supported by a University of Otago Division of Health Sciences Career Development Postdoctoral Fellowship. Other funding for this project was provided by an Otago University Research grant to J.E.-R.

Appendix A. Supplementary data

Supplementary data associated with this article can be found, in the online version, at http://dx.doi.org/10.1016/j.febslet.2014.08.024.

References

[1] Vinyard, D.J., Ananyev, G.M. and Dismukes, G.C. (2013) Photosystem II: the reaction center of oxygenic photosynthesis. Annu. Rev. Biochem. 82, 577–606.
[2] Umena, Y., Kawakami, K., Shen, J.-R. and Kamiya, N. (2011) Crystal structure of oxygen-evolving Photosystem II at a resolution of 1.9 Å. Nature 473, 55–60.
[3] Vass, I. (2011) Role of charge recombination processes in photodamage and photoprotection of the Photosystem II complex. Physiol. Plant 142, 6–16.
[4] Tyystjärvi, E. (2013) Photoinhibition of Photosystem II. Int. Rev. Cell Mol. Biol. 300, 243–303.
[5] Nickelsen, J. and Rengstl, B. (2013) Photosystem II assembly: from cyanobacteria to plants. Annu. Rev. Plant Biol. 64, 609–635.
[6] Nixon, P.J., Michoux, F., Yu, J., Boehm, M. and Komenda, J. (2010) Recent advances in understanding the assembly and repair of Photosystem II. Ann. Bot. 106, 1–16.
[7] Mabbitt, P.D., Wilbanks, S.M. and Eaton-Rye, J.J. (2014) Structure and function of the hydrophilic Photosystem II assembly proteins: Psb27, Psb28 and Ycf48. Plant Physiol. Biochem. 81, 96–107.
[8] Plucken, H., Muller, B., Grohmann, D., Westhoff, P. and Eichacker, L.A. (2002) The HCF136 protein is essential for assembly of the Photosystem II reaction center in *Arabidopsis thaliana*. FEBS Lett. 532, 85–90.
[9] Komenda, J., Nickelsen, J., Tichý, M., Prášil, O., Eichacker, L.A. and Nixon, P.J. (2008) The cyanobacterial homologue of HCF136/YCF48 is a component of an early Photosystem II assembly complex and is important for both the efficient assembly and repair of Photosystem II in *Synechocystis* sp. PCC 6803. J. Biol. Chem. 283, 22390–22399.
[10] Rengstl, B., Oster, U., Stengel, A. and Nickelsen, J. (2011) An intermediate membrane subfraction in cyanobacteria is involved in an assembly network for Photosystem II biogenesis. J. Biol. Chem. 286, 21944–21951.
[11] Nowaczyk, M.M., Hebeler, R., Schlodder, E., Meyer, H.E., Warscheid, B. and Rögner, M. (2006) Psb27, a cyanobacterial lipoprotein, is involved in the repair cycle of Photosystem II. Plant Cell 18, 3121–3131.
[12] Grasse, N., Mamedov, F., Becker, K., Styring, S., Rögner, M. and Nowaczyk, M.M. (2011) Role of novel dimeric Photosystem II (PSII)-Psb27 protein complex in PSII repair. J. Biol. Chem. 286, 29548–29555.
[13] Komenda, J., Knoppová, J., Kopecná, J., Sobotka, R., Halada, P., Yu, J., Nickelsen, J., Boehm, M. and Nixon, P.J. (2012) The Psb27 assembly factor binds to the CP43 complex of Photosystem II in the cyanobacterium *Synechocystis* sp. PCC 6803. Plant Physiol. 158, 476–486.
[14] Chen, H., Zhang, D., Guo, J., Wu, H., Jin, M., Lu, Q., Lu, C. and Zhang, L. (2006) A Psb27 homologue in *Arabidopsis thaliana* is required for efficient repair of photodamaged Photosystem II. Plant Mol. Biol. 61, 567–575.
[15] Mamedov, F., Nowaczyk, M.M., Thapper, A., Rögner, M. and Styring, S. (2007) Functional characterization of monomeric Photosystem II core preparations from *Thermosynechococcus elongatus* with or without the Psb27 protein. Biochemistry 46, 5542–5551.
[16] Liu, H., Huang, R.Y., Chen, J., Gross, M.L. and Pakrasi, H.B. (2011) Psb27, a transiently associated protein, binds to the chlorophyll binding protein CP43 in Photosystem II assembly intermediates. Proc. Natl. Acad. Sci. USA 108, 18536–18541.
[17] Liu, H., Roose, J.L., Cameron, J.C. and Pakrasi, H.B. (2011) A genetically tagged Psb27 protein allows purification of two consecutive Photosystem II (PSII) assembly intermediates in *Synechocystis* 6803, a cyanobacterium. J. Biol. Chem. 286, 24865–24871.
[18] Mabbitt, P.D., Eaton-Rye, J.J. and Wilbanks, S.M. (2013) Mutational analysis of the stability of Psb27 from *Synechocystis* sp. PCC 6803: implications for models of Psb27 structure and binding to CP43. Eur. Biophys. J. 42, 787–793.
[19] Roose, J.L. and Pakrasi, H.B. (2008) The Psb27 protein facilitates manganese cluster assembly in Photosystem II. J. Biol. Chem. 283, 4044–4050.
[20] Bricker, T.M., Roose, J.L., Fagerlund, R.D., Frankel, L.K. and Eaton-Rye, J.J. (2012) The extrinsic proteins of Photosystem II. Biochim. Biophys. Acta 1817, 121–142.
[21] Liu, H., Chen, J., Huang, R.Y., Weisz, D., Gross, M.L. and Pakrasi, H.B. (2013) Mass spectrometry-based footprinting reveals structural dynamics of loop E of the chlorophyll-binding protein CP43 during Photosystem II assembly in the cyanobacterium *Synechocystis* 6803. J. Biol. Chem. 288, 14212–14220.
[22] Li, M.Z. and Elledge, S.J. (2007) Harnessing homologous recombination in vitro to generate recombinant DNA via SLIC. Nat. Methods 4, 251–256.
[23] Hill, R.E. and Eaton-Rye, J.J. (2014) Plasmid construction by SLIC or sequence and ligation-independent cloning. Methods Mol. Biol. 1116, 25–36.
[24] Prentki, P. and Krisch, H.M. (1984) In vitro insertional mutagenesis with a selectable DNA fragment. Gene 29, 303–313.
[25] Williams, J.G.K. (1988) Construction of specific mutations in Photosystem-II photosynthetic reaction center by genetic-engineering methods in *Synechocystis*-6803. Methods Enzymol. 167, 766–778.
[26] Morris, J.N., Crawford, T.S., Jeffs, A., Stockwell, P.A., Eaton-Rye, J.J. and Summerfield, T.C. (2014) Whole genome re-sequencing of two 'wild-type' strains of the model cyanobacterium *Synechocystis* sp. PCC 6803. New Zeal. J. Bot. 52, 36–47.
[27] Eaton-Rye, J.J. (2011) Construction of gene interruptions and gene deletions in the cyanobacterium *Synechocystis* sp. strain PCC 6803. Methods Mol. Biol. 684, 295–312.
[28] MacKinney, G. (1941) Absorption of light by chlorophyll solutions. J. Biol. Chem. 140, 315–322.
[29] Cser, K. and Vass, I. (2007) Radiative and non-radiative charge recombination pathways in Photosystem II studied by thermoluminescence and chlorophyll fluorescence in the cyanobacterium *Synechocystis* 6803. Biochim. Biophys. Acta 1767, 233–243.
[30] Joliot, A. and Joliot, P. (1964) Etude cinétique de la réaction photochimique libérant l'oxygène au cours de la photosynthèse. C. R. Acad. Sci. Paris 258, 4622–4625.
[31] Mitschke, J., Georg, J., Scholz, I., Sharma, C.M., Dienst, D., Bantscheff, J., Voss, B., Steglich, C., Wilde, A., Vogel, J. and Hess, W.R. (2011) An experimentally anchored map of transcriptional start sites in the model cyanobacterium *Synechocystis* sp. PCC6803. Proc. Natl. Acad. Sci. USA 108, 2124–2129.
[32] Calderon, R.H., Garcia-Cerdan, J.G., Malnoe, A., Cook, R., Russell, J.J., Gaw, C., Dent, R.M., de Vitry, C. and Niyogi, K.K. (2013) A conserved rubredoxin is necessary for Photosystem II accumulation in diverse oxygenic photoautotrophs. J. Biol. Chem. 288, 26688–26696.
[33] Bentley, F.K., Luo, H., Dilbeck, P., Burnap, R.L. and Eaton-Rye, J.J. (2008) Effects of inactivating *psbM* and *psbT* on photodamage and assembly of Photosystem II in *Synechocystis* sp. PCC 6803. Biochemistry 47, 11637–11646.
[34] Burnap, R.L., Troyan, T. and Sherman, L.A. (1993) The highly abundant chlorophyll-protein complex of iron-deficient *Synechococcus* sp. PCC7942 (CP43′) is encoded by the *isiA* gene. Plant Physiol. 103, 893–902.
[35] Boehm, M., Romero, E., Reisinger, V., Yu, J., Komenda, J., Eichacker, L.A., Dekker, J.P. and Nixon, P.J. (2011) Investigating the early stages of Photosystem II assembly in *Synechocystis* sp. PCC 6803: isolation of CP47 and CP43 complexes. J. Biol. Chem. 286, 14812–14819.
[36] Strasser, R.J., Srivastava, A. and Govindjee (1995) Polyphasic chlorophyll *a* fluorescence transient in plants and cyanobacteria. Photochem. Photobiol. 61, 32–42.
[37] Hwang, H.J., Nagarajan, A., McLain, A. and Burnap, R.L. (2008) Assembly and disassembly of the Photosystem II manganese cluster reversibly alters the coupling of the reaction center with the light-harvesting phycobilisome. Biochemistry 47, 9747–9755.
[38] Boehm, M., Yu, J., Reisinger, V., Beckova, M., Eichacker, L.A., Schlodder, E., Komenda, J. and Nixon, P.J. (2012) Subunit composition of CP43-less Photosystem II complexes of *Synechocystis* sp. PCC 6803: implications for the assembly and repair of Photosystem II. Philos. Trans. R. Soc. B 367, 3444–3454.

[39] Komenda, J., Sobotka, R. and Nixon, P.J. (2012) Assembling and maintaining the Photosystem II complex in chloroplasts and cyanobacteria. Curr. Opin. Plant Biol. 15, 245–251.
[40] Knoppová, J., Sobotka, R., Tichý, M., Yu, J., Konik, P., Halada, P., Nixon, P.J. and Komenda, J. (2014) Discovery of a chlorophyll binding protein complex involved in the early steps of Photosystem II assembly in *Synechocystis*. Plant Cell 26, 1200–1212.
[41] Rengstl, B., Knoppova, J., Komenda, J. and Nickelsen, J. (2013) Characterization of a *Synechocystis* double mutant lacking the Photosystem II assembly factors YCF48 and Sll0933. Planta 237, 471–480.
[42] Vass, I., Kirilovsky, D. and Etienne, A.L. (1999) UV-B radiation-induced donor- and acceptor-side modifications of Photosystem II in the cyanobacterium *Synechocystis* sp. PCC 6803. Biochemistry 38, 12786–12794.
[43] Faller, P., Fufezan, C. and Rutherford, A.W. (2005) Side-path electron donors: cytochrome b_{559}, chlorophyll Z and β-carotene, in: Photosystem II: The Light-Driven Water:Plastoquinone Oxidoreductase (Wydrzynski, T. and Satoh, K., Eds.), Advances in Photosynthesis and Respiration, vol. 22, pp. 347–365, Springer, Dordrecht.
[44] Wilson, A., Punginelli, C., Gall, A., Bonetti, C., Alexandre, M., Routaboul, J.M., Kerfeld, C.A., Van Grondelle, R., Robert, B., Kennis, J.T. and Kirilovsky, D. (2008) A photoactive carotenoid protein acting as light intensity sensor. Proc. Natl. Acad. Sci. USA 105, 12075–12080.